Colliding Beam Fusion Reactor

N. Rostoker, M.W. Binderbauer and F.J. Wessel
University of California, Irvine, CA 92697

H.J. Monkhorst
University of Florida, Gainesville, FL 32611

Abstract

Conceptual reactor designs are investigated that are based on the Field Reversed Configuration for D-$He^3$and p-B^{11} reactions. The majority of fuel ions have a sufficiently large orbit size in the FRC so that classical transport should prevail in the absence of long wavelength instabilities. We consider a first mode of operation wherein the mean azimuthal velocities and temperatures of the two ion species are the same and the current is not neutralized by electrons. The distribution functions are thermal in a moving frame of reference. In this mode the energy invested in the ion beams increases the circulating power. The return on this investment is current drive and and avoidance of anomalous transport. In the second mode of operation the two ion species have different azimuthal velocities selected to take advantage of the resonance in the fusion cross section. This leads to a larger reactivity and a further increase in circulating power with a net gain in power for sale. Power flow calculations will be presented based on anticipated conversion efficiencies for charged particles and radiation.

1. Motivation: Classical Confinement of Ions

A plasma consisting of large orbit ions and small orbit electrons is considered. Experimental evidence[1] with energetic beams injected into Tokamaks for heating in DIII-D and TFTR and with energetic fusion products in JET indicates that such a plasma may not suffer from the anomalous transport characteristics usually observed in fusion devices. In fact the diffusion of these large orbit ions is consistent with classical estimates while at the same time the thermal population diffuses anomalously. In addition to Tokamak experiments numerical simulations[2] support the fact that large orbit particles respond predominantly to low frequency field fluctuations with wavelengths that exceed the larmor radius. The physical reason for this is that ions, over the course of their orbit, average the fluctuations so that only long wavelengths (compared to gyro-radius) and small frequencies (compared to gyro-frequency) cause transport. Thus if the particle orbit radius is large and the plasma has gross stability at long wavelengths, anomalous transport can in principle be avoided.[3]

[1]W.W. Heidbrink and G.J. Sadler, *Nucl. Fusion* **34**, 535, 1994.

[2]H. Naitou, T. Kamimura, and J. Dawson, *J. Phys. Soc. Jpn.* **46**, 258, 1997; G. Manfredi and R.O. Dendy, *Phys. Rev. Lett.* **76**, 4360, 1996.

[3]M.W. Binderbauer and N. Rostoker, *J. Plasma Phys.* **56**, 451, 1996.

2. Conceptual Reactor Design

The basis of the design for the reactor discussed in this paper is the Field Reversed Configuration (FRC) illustrated in Figs. 1 and 2. This choice is made because it is the only confinement system studied to date where a substantial fraction of the ions have large orbits so that the possible elimination of anomalous transport can be studied.

Experiments were carried out at Los Alamos where the ratio of the plasma scale size to the mean ion gyro-radius[4] was typically $s \simeq 2$. These experiments were carried out over a period of about 12 years and were terminated by DOE about 7 years ago.

Currently, there is an experimental program at the University of Washington. The objective is to achieve $s \geq 10$ which is considered necessary for a reactor. The current is to be carried by electrons driven by a rotating magnetic field.

In this paper we consider a modified[5] FRC where $s \leq 2$ and the current is carried by energetic ions. In a reactor the energetic ions would be supplied by external accelerators that produce beams that consist of neutrals or ions with neutralizing electrons. The beams could be steady state or repetitively pulsed. They would be injected and trapped continuously to replace fuel ions as they react and also to maintain the current. In this paper repetitively pulsed beams will be emphasized because the technology is closer to feasibility.

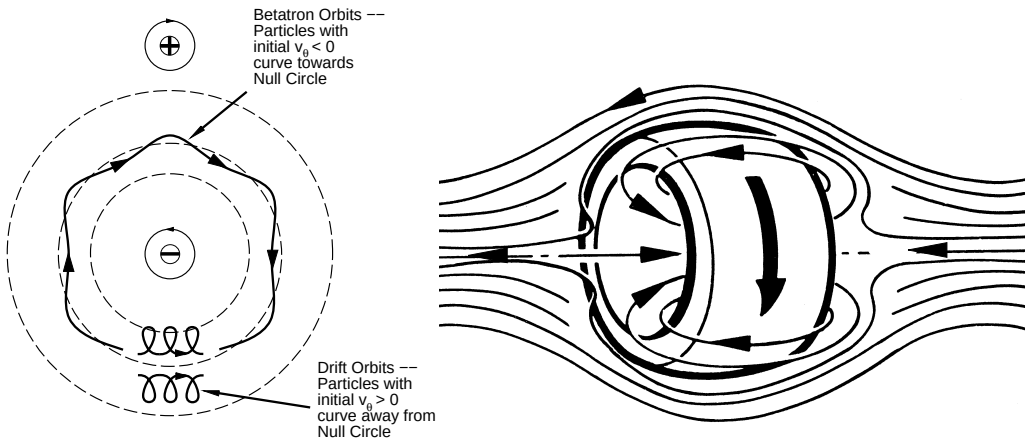

Figure 1: Field Reversed Configuration with typical particle orbits

3. Stability

Plasma physics in the past 45 years has produced an endless list of instabilities. However, the treatments are usually for low beta, slowly varying magnetic fields, small orbit radius particles, etc. None of these conditions apply to the CBFR. The magneto-hydrodynamic approximation is the most widely employed treatment of instabilities in confinement devices. For the FRC it predicts for example the tilt mode which would destroy confinement in a few microseconds. It is not observed except in large s experiments. Understanding the FRC stability requires new theories[6] that consider high beta, large gyro-radius, and magnetic

[4] M. Tuszewski, *Nucl. Fusion* **28**, 2033, 1988.
[5] N. Rostoker *et al.*, *Phys. Rev. Lett.* **70**, 1818, 1993.
[6] M. Binderbauer, PhD thesis, UC Irvine, 1996.

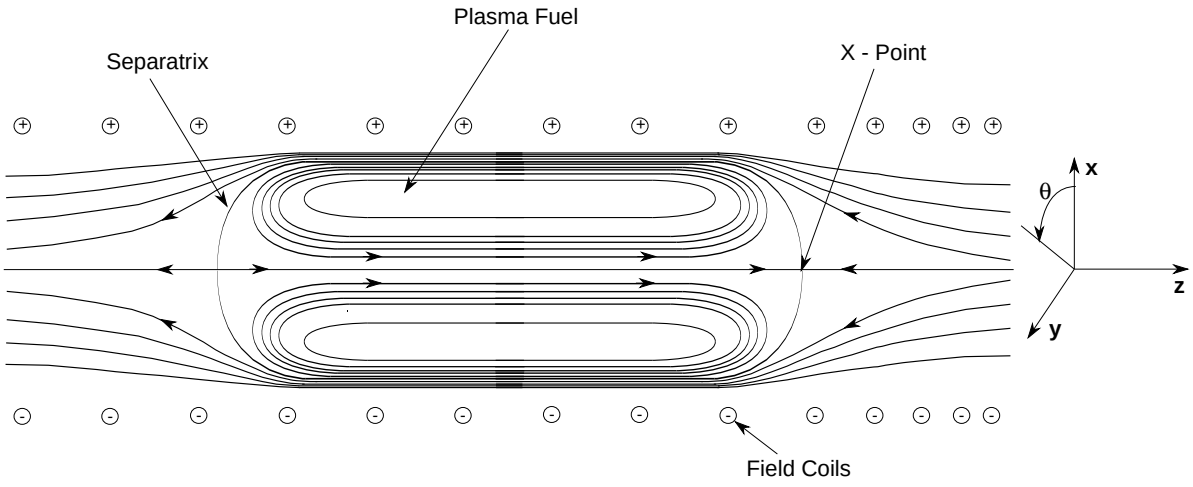

Figure 2: Flux surfaces for a typical FRC

fields that have null surfaces, x-points, etc. Long wavelength stability will be assumed in the balance of this paper.

4. Physics and Engineering Analysis

4.1 Physics Analysis

In order to describe the injection and trapping of particle beams as well as fusion reactions and diffusion it is necessary to add sources and sinks to the Vlasov/Fokker-Planck equation[7]

$$\frac{\partial f_i}{\partial t}+\mathbf{v}\cdot\frac{\partial fi}{\partial \mathbf{x}}+\frac{e_i}{m_i}\left(\mathbf{E}+\frac{1}{c}\mathbf{v}\times\mathbf{B}\right)\cdot\frac{\partial f_i}{\partial \mathbf{v}}=-\frac{\partial}{\partial \mathbf{v}}\langle\Delta\mathbf{v}\rangle_i f_i+\frac{1}{2}\frac{\partial}{\partial \mathbf{v}}\cdot\frac{\partial}{\partial \mathbf{v}}\langle\Delta\mathbf{v}\Delta\mathbf{v}\rangle_i f_i+Q_i-S_i \quad (1)$$

Q_i is the source due to beam injection and trapping. S_i is the sink due to fusion of fuel ions. $f_i(\mathbf{x},\mathbf{v};t)$ is the distribution function for particles of type i which includes electrons, two types of fuel ions and fusion product ions. A less complete description is produced by moment equations which are multi-fluid equations.

$$\frac{\partial n_i}{\partial t}+\boldsymbol{\nabla}\cdot n_i\mathbf{V}_i=0 \quad (2)$$

and

$$n_i m_i\frac{d\mathbf{V}_i}{dt}=n_i e_i\left(\mathbf{E}+\frac{1}{c}\mathbf{V}_i\times\mathbf{B}\right)-\boldsymbol{\nabla}(n_iT_i)+n_im_i\sum_{k\neq i}\frac{\mathbf{V}_k-\mathbf{V}_i}{t_{ik}}\ . \quad (3)$$

$$\frac{d}{dt}=\frac{\partial}{\partial t}+\mathbf{V}_i\cdot\boldsymbol{\nabla}\qquad\text{and}\qquad n_i\mathbf{V}=\int f_i\mathbf{v}d\mathbf{v}\ .$$

n_i is density and $\mathbf{V}_i$ is fluid velocity; t_{ik} are momentum exchange times between particles i and k. Momentum conservation requires that

$$\frac{n_im_i}{t_{ik}}=\frac{n_km_k}{t_{ki}}\ . \quad (4)$$

[7]Expressions for the Fokker-Planck coefficients may be found in M.N. Rosenbluth, W.M. MacDonald and D.L. Judd, *Phys. Rev.* **107**, 1, 1957.

For example

$$t_{ei} = \frac{3}{8}\sqrt{\frac{\pi}{2}}\frac{T_e^{3/2}m^{1/2}}{n_i Z_i^2 e^4 \ln\Lambda} \ , \tag{5}$$

$$t_{ie} = \frac{n_i m_i}{n_e m} t_{ei} \ .$$

Unless otherwise noted it will be assumed that all distribution functions are of the form

$$f_i(\mathbf{x},\mathbf{v};t) = n_i(r,t)\left(\frac{m_i}{2\pi T_i}\right)^{3/2}\exp\left[-\frac{m_i}{2T_i}(\mathbf{v}-\mathbf{V}_i)^2\right] \ , \tag{6}$$

i.e.: they are drifted Maxwell distributions where T_i and V_i may be time dependent. The justification for this assumption is that the self-collision or Maxwellization times are short compared to other times

$$t_{ee} = \frac{m^{1/2}T^{3/2}}{4\pi n e^4 \ln\Lambda} \simeq \frac{10^9 T^{3/2}}{n} \simeq 10^{-3} \text{ sec} \tag{7}$$

$$t_{ii} \simeq \sqrt{\frac{m_i}{m}} t_{ee} \simeq .06 \text{ sec}$$

assuming $n \simeq 10^{15}$ cm^{-3} and $T = 100$ keV. The momentum exchange time t_{ie} is of order 1 sec. However, t_{ei} is of the same order as t_{ee}. The effective slowing down times may be extended substantially by inductive effects. Nevertheless the justification for this approximation is not always adequate and will be noted.

We will usually assume axial symmetry and that the plasma is infinite in the axial direction. From axial symmetry it can be shown[8] from Eqs. (2) and (3) that

$$P_\theta = \sum_i \int_{r=0}^{r=r_B} 2\pi r dr \left[mrV_{i\theta} + \frac{e_i}{c} r A_\theta\right] n_i = \text{constant} \ . \tag{8}$$

$A_\theta(r,t)$ is the vector potential. Another approximation is quasi-neutrality according to which

$$\sum_i e_i n_i = 0$$

so that mechanical momentum is conserved. Further reduction of Eqs. (2) and (3) leads to the conservation of energy

$$\frac{d}{dt}\left[\sum_i\left(\frac{1}{2}N_i m_i V_{i\theta}^2\right) + \frac{1}{2}LI^2\right] = \sum_{k\neq i}\frac{N_i m_i}{\tau_{ik}} V_{i\theta}(V_{k\theta} - V_{i\theta}) = -I^2 R \ , \tag{9}$$

where

$$I = \frac{1}{2\pi r_o}\sum_i N_i e_i V_{i\theta} \ ,$$

$$R = \frac{(2\pi r_o)^2 m}{N_e e^2}\left[\frac{1}{\tau_{e1}} + \frac{1}{\tau_{e2}}\right]$$

[8] N. Rostoker and A.C. Kolb, *Phys. Fluids* **5**, 1962.

and

$$N_i = \int_{r=0}^{r=r_B} 2\pi r\, dr\, n_i \ .$$

An electric field $E_\theta = -(L/2\pi r_o)(dI/dt)$ has been assumed. The velocity $\mathbf{V}_i$ has components $V_{i\theta}$ and V_{ir} where $V_{i\theta} \gg V_{ir}$. τ_{ik} differs from t_{ik} by a numerical factor of order unity that derives from the r-integration.

The temperatures are defined as follows

$$\frac{3}{2} N_j T_j(t) = \int 2\pi r\, dr \int d\mathbf{v} f_j(r, \mathbf{v}; t) \frac{1}{2} m_j (\mathbf{v} - \mathbf{V}_j)^2 \tag{10}$$

with

$$N_j \mathbf{V}_j = \int 2\pi r\, dr \int d\mathbf{v} f_j(r, \mathbf{v}; t)\, \mathbf{v} \ .$$

From the appropriate moments of Eqs. (2) and (3)

$$\begin{aligned} \frac{3}{2} n_{io} \frac{dT_i}{dt} &= m_i \int 2\pi r\, dr \int d\mathbf{v} \left[(\mathbf{v} - \mathbf{V}_i) \langle \Delta \mathbf{v} \rangle_i + \frac{1}{2} \operatorname{tr} \langle \Delta \mathbf{v} \Delta \mathbf{v} \rangle_i \right] f_i \\ &= \frac{8\pi}{3} \gamma \sum_{j \neq i} n_{jo} Z_i^2 Z_j^2 e^4 \ln \Lambda \left\{ \frac{1}{m_i |V_i - V_j|} \operatorname{erf} \frac{|V_i - V_j|}{\sqrt{2}(v_i^2 + v_j^2)^{1/2}} \right. \\ &\quad \left. - \left(\frac{1}{m_i} + \frac{1}{m_j} \right) \frac{4\pi v_i^2}{[2\pi(v_i^2 + v_j^2)]^{3/2}} \exp \left[-\frac{1}{2} \frac{|V_i - V_j|}{(v_i^2 + v_j^2)} \right] \right\} \ . \end{aligned} \tag{11}$$

Drifted Maxwell distribution functions have been assumed; $T_i = m_i v_i^2$; γ is a numerical factor of order unity that results from the calculation

$$\int_0^{r_B} n_i(r) n_j(r) 2\pi r\, dr = \gamma n_{io} n_{jo} 2\pi r_o \Delta r$$

where n_{io}, n_{jo} are the maximum values and $2\pi r_o \Delta r$ is defined so that $N_i = \int_0^{r_B} n_i(r) 2\pi r dr = n_{io} 2\pi r_o \Delta r$. Eqs. (2), (3), (9) and (11) facilitate the determination of density n_i, mean velocity $\mathbf{V}_i$ and temperature when sources and sinks have been specified. The starting point is equilibrium fluid equations which are a reduction of Eqs. (2) and (3) that do not include collisions, sources or sinks. The basic equations are

$$-n_j m_j r \omega_j^2 = n_j e_j \left(E_r + \frac{r\omega_j}{c} B_z \right) - T_j \frac{dn_j}{dr} \ , \tag{12}$$

$$n_e = \sum_i n_i Z_i e$$

and

$$\frac{dB_z}{dr} = -\frac{4\pi e r}{c} \left[\sum_i n_i Z_i \omega_i - n_e \omega_e \right] \ . \tag{13}$$

These equations derive from rigid rotor Maxwell distributions where $V_{i\theta} = r\omega_i$.

4.2 Engineering Analysis

Power flow for the fusion reactor cycle of a CBFR is illustrated in Fig. 3. Definitions of the various quantities are as follows:

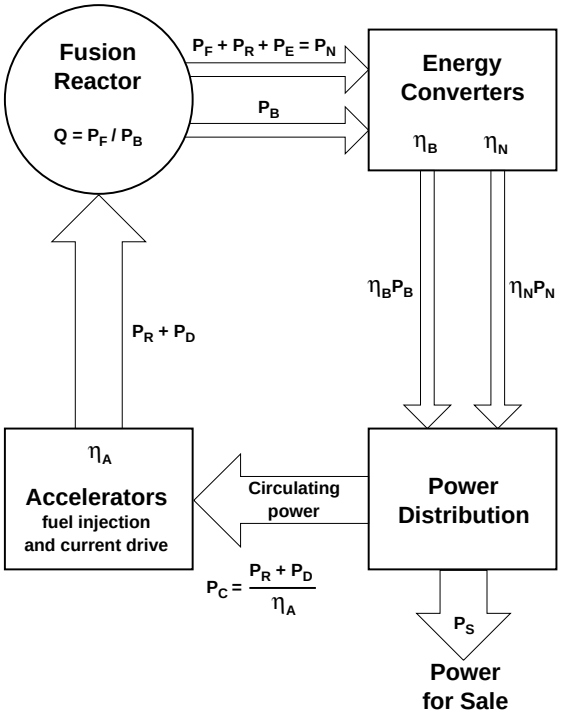

Figure 3: Power Flow Schematic

Fusion power density

$$P_F = 1.6 \times 10^{-19} n_1 n_2 \epsilon_F \langle \sigma v \rangle \text{ W/cm}^3 \tag{14}$$

n_1, n_2 are the fuel densities in cm^{-3}. ϵ_F is the fusion energy released by a fusion reaction in electron volts and $\langle \sigma v \rangle$ is the fusion reactivity in cm^3/sec.

Bremsstrahlung

$$\begin{aligned} P_B &= 1.5 \times 10^{-32} \langle Z \rangle \, n_e^2 \, T_e^{1/2} \left\{ 1 + 1.78 \left(\frac{T_e}{mc^2} \right)^{1.34} \right. \\ &\left. + \frac{2.12}{\langle Z \rangle} \left(\frac{T_e}{mc^2} \right) \left[1 + 1.1 \left(\frac{T_e}{mc^2} \right) + \left(\frac{T_e}{mc^2} \right)^2 - 1.25 \left(\frac{T_e}{mc^2} \right)^{2.5} \right] \right\} \text{ W/cm}^3 \, . \end{aligned} \tag{15}$$

This formula by Svensson[9] is the most accurate in the range 50 keV$\leq T_e \leq$200 keV. n_e is the electron density in cm^{-3}, T_e is electron temperature in electron volts and $\langle Z \rangle = \sum_i n_i Z_i^2 / \sum_i n_i Z_i$ where the sum is over fuel ions.

Dissipation of fuel ion energy

$$P_D = \frac{I^2 R}{2\pi r_o \Delta r \gamma} = \frac{n_{1o} m_1}{t_{1e}} (V_1 - V_e)^2 + \frac{n_{2o} m_2}{t_{2e}} (V_2 - V_e)^2$$

and $P_R = (\epsilon_1 + \epsilon_2) n_1 n_2 \langle \sigma v \rangle \times 1.6 \times 10^{-19}$ W/cm^3 is the average power density of the beams required to replace the fuel ions at their design energy. ϵ_1, ϵ_2 are beam energies in electron volts.

[9] R. Svensson, *Astro. Phys. J.* **258**, 335, 1982.

P_E = power density carried by escaping electrons which accompany the fusion products when they leave the reaction chamber.

$P_N = P_F + P_R + P_E$
This is the power density of escaping particles that can be converted with high efficiency.

P_P = heating of fuel ions by fusion product ions.

$Q = P_F/P_B$ is a figure of merit.

P_C = circulating power provided by accelerators to replace fuel ions and losses to maintain the current.

P_S = output power density for sale.

η_B = efficiency of conversion of Bremsstrahlung power.

η_A = accelerator efficiency.

η_N = efficiency of conversion of power associated with charged particles.

Relations among these quantities are

$$P_S = \eta_B P_B + \eta_N P_N - P_C \ ,$$

$$P_C = \frac{P_R + P_D}{\eta_A} \ .$$

The heating of fuel ions by fusion product ions reduces the circulating power as well as the output power due to fusion product ions, i.e.: this power is consumed internally.

$$\frac{P_S}{P_F} = \frac{\eta_B}{Q} + \eta_N \left[1 + \frac{P_R + P_E - P_P}{P_F}\right] - \frac{P_R + P_D}{\eta_A P_F} \ . \tag{16}$$

$$\frac{P_C}{P_F} = \frac{P_R + P_D}{\eta_A P_F} \ . \tag{17}$$

5. FRC Equilibrium

For electrons and a single ion type Eqs. (12) and (13) have an exact solution.[5]

$$n_e(r) = \frac{n_{eo}}{\cosh^2\left[(r^2 - r_o^2)/r_o\Delta r\right]} = n_i(r) \tag{18}$$

and

$$B_z(r) = -B_o\left[1 + \sqrt{\beta}\tanh\left(\frac{r^2 - r_o^2}{r_o\Delta r}\right)\right] \ . \tag{19}$$

r_o is the radius at which the density is a maximum. The directions of the magnetic field are indicated in Fig. 2.

$$r_o \Delta r = 2\sqrt{2} \left(\frac{T_e + T_i}{4\pi n_{eo} e^2} \right)^{1/2} \frac{c}{|\omega_i - \omega_e|} \tag{20}$$

and

$$\beta = 8\pi n_{eo} \frac{T_e + T_i}{B_o^2} \ . \tag{21}$$

n_{eo} is the electron density maximum and $-B_o$ is the externally applied magnetic field. There is a substantial electric field that is confining for electrons

$$E_r = -\frac{V_e}{c} B_z - \frac{T_e}{e n_e} \frac{dn_e}{dr} \ , \tag{22}$$

$V_e = r\omega_e$ and $V_i = r\omega_i$. The ion velocity is determined by the ion energy created by an external accelerator. The maximum particle density may also be determined by design. The temperatures cannot be determined from the Vlasov-Maxwell equations. Higher order processes must be included – Coulomb collisions as well as particle sources and sinks. Other features of the higher order processes have already been included such as the assumption of drifted Maxwell distributions for electrons and ions which must be verified a posteriori. The external magnetic field B_o and V_e can be identified by considering the conservation of momentum of a single fluid description

$$\rho \frac{V_\theta^2}{r} = \frac{\partial}{\partial r} \left(P + \frac{B_z^2}{8\pi} \right) \ ,$$

where $\rho V_\theta = \sum_i m_i \int f_i \mathbf{v}\, d\mathbf{v} = \sum_j n_j m_j r \omega_j$ and $\rho = \sum_j n_j m_j \simeq n_i m_i$ since $m_i \gg m$. Eq. (22) can be integrated from $r = 0$ to $r = r_B = \sqrt{2} r_o$. At these limits $P = n_{eo}(T_e + T_i) \simeq 0$ so that

$$\int_0^{r_B} \rho \frac{V_\theta^2}{r} dr = m_i \omega_i^2 \int_0^{r_B} n_i r \, dr = r_o \Delta r n_{io} m_i \omega_i^2 \ .$$

Additionally assuming $r_o \gg \Delta r$

$$\int_0^{r_B} \frac{\partial}{\partial r} \frac{B_z^2}{8\pi} dr = \frac{1}{8\pi} \left[(B_o + B_m)^2 - (B_o - B_m)^2 \right] = \frac{1}{2\pi} B_o B_m \ ,$$

where $B_m = \sqrt{8\pi n_{eo}(T_e + T_i)}$. Substituting Eq. (20) for $r_o \Delta r$ the result is

$$\omega_e = \omega_i \left[1 - \frac{\omega_i}{\Omega_o} \right] \ , \tag{23}$$

where $\Omega_o = eB_o / m_i c$ is the ion cyclotron frequency in the externally applied field B_o. Since $V_i = r\omega_i$ is determined by a design choice, Eq. (23) determines the mean electron velocity $V_e = r\omega_e$, i.e.:

$$V_e = V_i \left[1 - \frac{\omega_i}{\Omega_o} \right] \ . \tag{24}$$

If $\omega_i = \Omega_o$, $V_e = 0$. By increasing the applied field B_o the value of V_e can be controlled and, therefore, the value of the plasma width Δr according to Eq. (20).

The FRC equilibrium serves as a starting point for kinetic analysis of a reactor model. With some approximations the solution described above can be adapted to a fuel with two different types of ions, one with $Z_1 = 1$ and one with $Z_2 \geq 1$ to accommodate the reactions D-T, D-He^3 and p-B^{11}. The approximation suggested by Coulomb collisions is that the fuel ions would have the same temperatures and velocities $V_i = r\omega_i$ because ion-ion collisions would lead to thermalization more rapidly than slowing down of ions or speeding up by electrons as discussed in Sec. 3. The previous equations for a single type fuel ion are modified as follows

$$r_o \Delta r = 2\sqrt{2} \left[\frac{T_e + [2T_i/(1+Z)]}{4\pi n_{eo} e^2} \right]^{1/2} \frac{c}{\omega_i - \omega_e} \ , \tag{25}$$

$$\beta = \frac{8\pi n_{eo}}{B_o^2} \left[T_e + \frac{2}{1+Z} T_i \right] \ , \tag{26}$$

and

$$\Omega_o = \frac{(n_{1o} + n_{2o} Z) e B_o}{n_{1o} m_1 + n_{2o} m_2} \ . \tag{27}$$

6. Analysis of FRC Experiments

The FRC is formed by the inductive or Θ-pinch[10] method which preferentially heats ions by compression. After the compression the current is carried by electrons and the ions have zero drift velocity and a temperature of about 500 eV. The electron temperature is about 100 eV. After reconnection there is a radial magnetic field at the ends as illustrated in Figs. 1 and 2. This field is focusing for ions that rotate in the diamagnetic direction and defocusing for rotation in the opposite direction. Projections of typical orbits are illustrated in Fig. 1. There is selective confinement. A substantial fraction of the ions are accelerated out of the plasma at the ends along with an equal number of electrons. The plasma acquires angular momentum as observed. The current would increase except that it is prevented from doing this by an inductive electric field that decelerates ions and accelerates electrons, the latter being much more important for limiting current increase. The net result is little change in current, but the plasma ends up rotating with about half the current carried by ions and half by electrons. Then the current decays due to dissipation. An equation for current decay is obtained by differentiating Eq. (9). It is

$$(L + L_I) \frac{dI}{dt} + IR = 0 \ . \tag{28}$$

$L \simeq (2\pi^2 r_o^2)/c^2$ is the inductance/unit length of the FRC.

$$L_I = \frac{(2\pi r_o)^2}{N_e e^2} \frac{m m_i}{m + m_i}$$

is the inertial inductance/unit length and $L_I \ll L$. The current is

$$I = \frac{e N_e}{2\pi r_o} (V_{i\theta} - V_{e\theta}) \tag{29}$$

[10] This analysis is based on information in the review paper: M. Tuszewski, *Nucl. Fusion* **28**, 2033, 1988.

and the current decay is mainly due to the increase in V_e. $N_i = N_e$ are line densities. Assuming experimental values of $T_e = 100$ eV and $n_e = 5 \times 10^{15}$ cm$^{-3} = n_i$, $\tau_{ei} = 3.9$ nsec and $\tau_{ie} = 7.02$ μsec according to Eq. (5).

$$R = \frac{(2\pi r_o)^2 m}{N_e e^2} \frac{1}{\tau_{ei}}$$

so that neglecting L_I the current decay time is

$$\frac{L}{R} = \frac{1}{4} \frac{r_o \Delta r}{(c/\omega_{pe})^2} \tau_{ei} \simeq 300 \ \mu\text{sec} \ . \tag{30}$$

We have assumed typical experimental values of $n_{eo} = 5 \times 10^{15}$ cm^{-3} and $r_o \Delta r = 40$ cm^2.

This result is consistent with observed lifetimes. The main point is that the inductive effect increases the decay time by many orders of magnitude. The time scale for slowing down of ions or speeding up of electrons is much larger than the thermalization times of electrons or ions given by Eq. (7). This justifies the basic approximations. In addition with $s \simeq 2$ anomalous transport should be reduced. Some anomalous transport is observed in the Los Alamos experiments.[10] However, there are experiments with larger compressions and smaller values of s where the classical diffusion[11] estimate of the lifetime is close to the observed values.

7. Modes of Operation of CBFRs

We consider fuel systems with two types of ions of mass m_1, m_2 and atomic number $Z_1 = 1$ and $Z_2 \geq 1$ such as D-T, D-He^{3}and p-B^{11}. The fusion cross section for each case has a resonance. The reactivity $\langle \sigma v \rangle$ can be calculated by

$$\langle \sigma v \rangle = \int d\mathbf{v}_1 d\mathbf{v}_2 F_1(\mathbf{v}_1) F_2(\mathbf{v}_2) |\mathbf{v}_1 - \mathbf{v}_2| \sigma(|\mathbf{v}_1 - \mathbf{v}_2|) \tag{31}$$

where

$$F_i(\mathbf{v}_i) = \left(\frac{m_i}{2\pi T_i}\right)^{3/2} \exp\left[-\frac{m_i}{2T_i}(\mathbf{v}_i - \mathbf{V}_i)^2\right] \ . \tag{32}$$

In the first mode of operation $\mathbf{V}_1 = \mathbf{V}_2$ and $T_1 = T_2$. The distribution functions are thermal in a moving frame of reference. The thermal reactivities designated in Fig. 4 are applicable and are the same as for a purely thermal reactor. V_1 and V_2 are large enough to avoid anomalous diffusion but as small as possible consistent with this to minimize the circulating power. The injection energy $\frac{1}{2}m_1 V_1^2 + \frac{1}{2}m_2 V_2^2$ is the price to be paid for avoiding anomalous diffusion. The advantages of this mode are that both fuel ions are in thermal equilibrium (ion–ion collisions assure this but do not contribute to transport), that there is no anomalous transport and that current drive is accomplished. In this paper we will only give examples for this mode since we are still in the process of evaluating the second mode discussed below.

The second mode of operation involves $\mathbf{V}_1 \neq \mathbf{V}_2$ and $\frac{1}{2}m_1(\mathbf{V}_1 - \mathbf{V}_2)^2 = \epsilon_R$ the resonant energy. The temperatures of the beams should be as low as possible to enhance the reactivity as illustrated in Fig. 4. In this case the steady state electron velocity would be $V_e = (n_1 V_1 +$

[11] Y. Asu, S. Himeno and K. Hirano, *Nucl. Fusion* **23**, 751, 1983.

$n_2 Z_2^2 V_2)/(n_1 + n_2 Z_2^2)$ where n_1, n_2 are fuel ion densities. The steady state current is the Ohkawa current

$$j_\theta = \frac{e n_1 n_2}{n_1 + n_2 Z_2^2}(Z_2^2 - Z_2)(V_1 - V_2) \ . \tag{33}$$

Provided that V_1 and V_2 can be maintained this takes care of current drive. If $Z_2 = 1$ as it is for D-T reactions $j_\theta = 0$. The resonance cannot be exploited for D-T reactions. However, it may be advantageous for the aneutronic reactions. Significant improvements in reactivity could be achieved with this mode if the beam temperatures can be kept below about 200 keV for p-B^{11} and 150 keV for D-He^3.

To achieve sustained reactions D.C. and pulsed accelerators have been considered. In this paper the emphasis will be on repetitively pulsed beams.

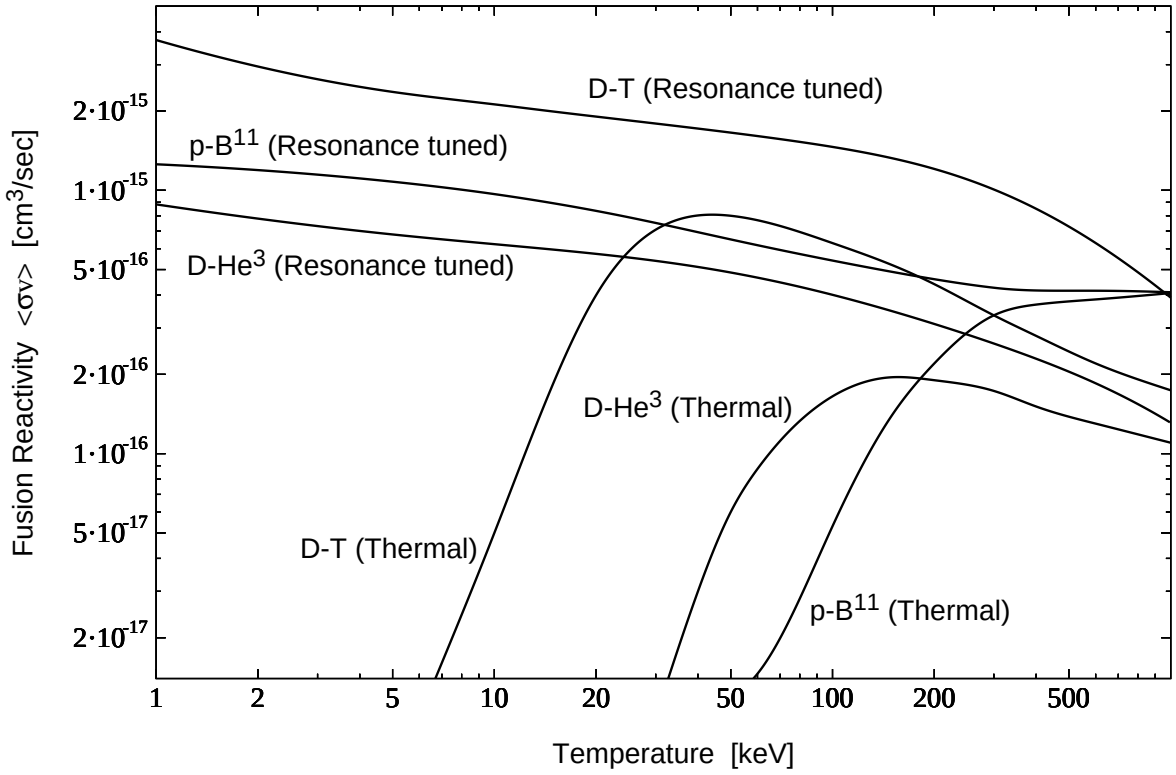

Figure 4: Various fusion reactivities.

7.1 CBFR – Mode 1

Current neutralization is an important consideration for an FRC. The question is on what time scale does it take place. When a beam is injected into a plasma with axial symmetry as illustrated in Fig. 5 the initial current increase induces an electric field E_θ which makes electrons drift in the radial direction, i.e.: $v_r = cE_\theta/B_z$. This electron drift changes the charge density producing a radial electric field in response to E_θ. The radial electric field

then produces a drift $v_\theta = -cE_r/B_z$ which could neutralize the beam current on a fast time scale. In fact such fast neutralization has never been observed. If there are open field lines electrons moving along the field lines would prevent the development of E_r. In this case current neutralization takes place on a collisional time scale which is L/R. If there is field reversal the magnetic field lines are closed and are equipotentials so that fast motion of electrons along field lines to prevent development of E_r is inhibited. It has been suggested[12] that fast neutralization can be prevented by breaking the symmetry with a quadrupole field or instabilities which permit electrons to move across field lines. In FRC's about half the current is carried by ions. There is no experimental evidence for fast neutralization with or without quadrupole windings. Electrons are sensitive to ubiquitous short wavelength turbulence so that they can cross field lines and prevent development of E_r on a fast time scale. In the present investigation we consider current neutralization to be on the collisional time scale.

Consider the injection of pulsed beams as illustrated in Fig. 6. The pulse duration $\Delta t \sim 10^{-6}$ sec is assumed to be short compared to the momentum transfer time $\tau_{ei} \sim 10^{-3}$ sec. The electron velocity $V_{e\theta}$ does not change during Δt as discussed above. During the period $(t_n + \Delta t,\ t_n + T)$ the current decays as described by Eq. (28). The decay time

$$\frac{L}{R} = \frac{1}{4}\frac{r_o \Delta r}{(c/\omega_{pe})^2}\left(\frac{\tau_{e1}\tau_{e2}}{\tau_{e1}+\tau_{e2}}\right) \tag{34}$$

is much greater than the τ_{ei}. During this time the ion velocities change very little; the current decay is almost entirely due to the change in electron velocity which involves very little energy change. The dissipated energy comes from the stored magnetic energy. From Eq. (9) we conclude that

$$\frac{1}{2}LI^2|_{t_n+\Delta t} - \frac{1}{2}LI^2|_{t_n+T} = I^2RT\ .$$

The loss of magnetic energy is replaced by the injected/trapped beam during the period $(t_{n+1},\ t_{n+1} + \Delta t)$. During this time which is much shorter that any of the momentum exchange times there is no significant effect from the Coulomb collisions of the injected beam ions on the fuel ions or vice versa. The injected/trapped beam replaces the fuel ions that are consumed by fusion reactions in the period $(t_n + \Delta t,\ t_n + T)$. The total number of fuel ions consumed and then supplied by the injected/trapped beam is

$$\Delta N_i = \frac{N_i}{\langle t_{Fi}\rangle}T \tag{35}$$

where $i = 1,\ 2$; $dn_i/dt = -n_1 n_2\langle\sigma v\rangle = dn_2/dt$. Eq. (35) is obtained by integrating these expressions. $t_{F1} = [n_2\langle\sigma v\rangle]^{-1}$ and $\langle t_{F1}\rangle = \frac{3}{2}[n_{2o}\langle\sigma v\rangle]^{-1}$ where the factor $\frac{2}{3}$ arises because the expressions on the right are bi-linear in density. The initial injected velocity is $V'_{i\theta} > V_{i\theta}$ so that the average velocity and the current are increased. This results in an inductive electric field $E_\theta = -(L/2\pi r_o)(dI/dt)$ that decelerates the ions and the energy lost by the

[12]H. Berk, H. Momota and T. Tajima, *Phys. Fluids* **30**, 3548, 1987; J.H. Hammer and H. Berk, *Nucl. Fusion* **22**, 89, 1982; A. Reimann and R.N. Sudan, *Comm. Plasma Phys. and Cont. Fusion* **5**, 167, 1979.

ions becomes magnetic energy. Integrating Eq. (9) from t_n to $t_n + \Delta t$ obtains the result

$$\begin{aligned}
&\sum_i \frac{1}{2} N_i m_i V_{i\theta}^2 \Big|_{t_n} - \frac{1}{2} N_i m_i V_{i\theta}^2 \Big|_{t_n+\Delta t} \\
&= \frac{1}{2} L I^2 \Big|_{t_n}^{t_n+\Delta t} \\
&= I^2 R T \\
&= \sum_i \frac{m_i}{2} \left(N_i(t_n + \Delta t) - \Delta N_i \right) V_{i\theta}^2 + \frac{m_i}{2} \Delta N_i (V'_{i\theta})^2 - \frac{m_i}{2} N_i(t_n + \Delta t) m_i V_{i\theta}^2 \ ,
\end{aligned}$$

$$\sum_i \frac{m_i}{2} \Delta N_i (V'_{i\theta})^2 = \sum_i \frac{m_i}{2} \Delta N_i V_{i\theta}^2 + I^2 R T \ . \tag{36}$$

The electron energy is much less than the ion energy and is omitted in the sums. Eq. (36) is the condition that the injected energy replaces the energy of the particles lost to fusion reactions and the dissipation from Coulomb collisions. $V_{i\theta}$ means the value at $t_n + \Delta t$ which does not change significantly in the period $(t_n + \Delta t,\ t_n + T)$. During this period the electron velocity $V_{e\theta}$ increases due to collisions that transfer momentum from the ions. However, in addition to this change in V_e

$$\frac{\Delta V_e}{V_i - V_e} = \frac{T}{L/R} \simeq 10^{-4} \ ,$$

there is a change in current due to the loss of electrons. $\Delta N_e = \sum_i \Delta N_i Z_i$ due to fusion. When fuel ions are consumed they are replaced by fusion product ions which must escape confinement and disappear at a similar rate in order to maintain a periodic or near steady state. These ions must take ΔN_e electrons with them in order to preserve charge neutrality. The current change is $eV_e \Delta N_e$ which is to be compared with $eN_e \Delta V_e$

$$\frac{V_e \Delta N_e}{N_e \Delta V_e} \simeq \frac{V_e}{V_i - V_e} \frac{L/R}{\langle t_{Fi} \rangle} \ .$$

This ratio can be greater or less than unity depending on the value of V_e. From the model equilibrium V_e can be related to the external magnetic field B_o. According to Eq. (24)

$$V_e = V_i \left[1 - \frac{\omega_i}{\Omega_o} \right]$$

where

$$\Omega_o = \frac{(n_{1o} + n_{2o} Z) e B_o}{(n_{1o} m_1 + n_{2o} m_2)} \ .$$

The change $V_e \Delta N_e$ during the period $(t_n + \Delta t,\ t_n + T)$ is compensated during the injection/trapping period $(t_n,\ t_n + \Delta t)$. An equal number ΔN_e of electrons is injected; the electron energy is small, but the equilibrium structure supports a drift velocity close to V_e. After many cycles a significant increase in V_e is possible. However, this could be compensated by a small decrease in B_o. This involves controlling small magnetic field changes on a long time scale of the order of seconds with a feedback system that follows the total current.

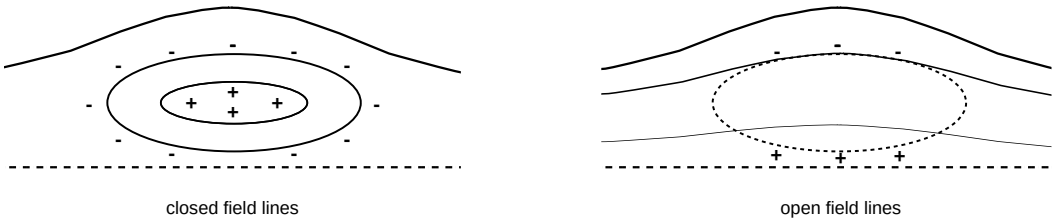

Figure 5: Current neutralization.

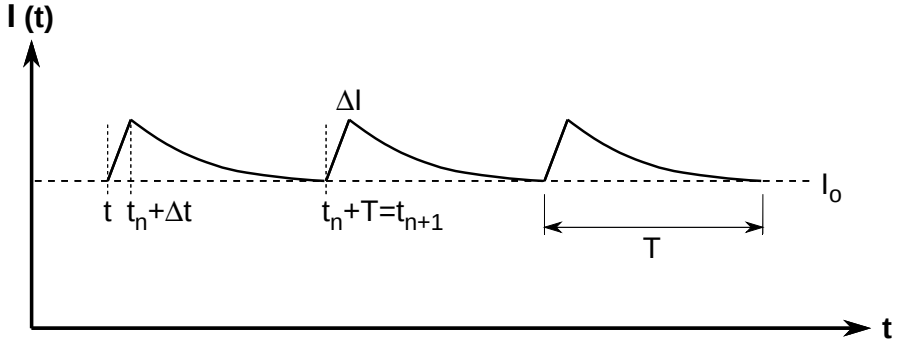

Figure 6: Pulsed beam injection after initial FRC formation.

8. Reactor Parameters - Mode 1

8.1 D-T Reactor

Consider the D-T reaction with the data as shown in Table 1.

Table 1: D-T Reactor Parameters

$n_{eo} = 10^{15}$ cm^{-3}	$n_{1o} = n_{2o} = .5 \times 10^{15}$ cm^{-3}
$\frac{1}{2} m_1 V_1^2 = 300$ keV	$\frac{1}{2} m_2 V_2^2 = 450$ keV
$\langle \sigma v \rangle = 1.2 \times 10^{-15}$ cm^3/sec	$t_{F1} = t_{F2} = 1/n_i \langle \sigma v \rangle = 1.67$ sec
$V_e = V_i \left[1 - \omega_i/\Omega_o\right] = .23 \times 10^9$ cm/sec	$V_1 = V_2 = .54 \times 10^9$ cm/sec
$r_o = 40$ cm	$B_o = 5.88$ kG
$\omega_1 = \omega_2 = 1.35 \times 10^7$ sec^{-1}	$\Omega_o = 2eB_o/(m_1 + m_2) = 2.35 \times 10^7$ sec^{-1}
$\epsilon_F = 17.4$ MeV	
(14 MeV neutrons, 3.4 MeV α-particles)	

$$r_o \Delta r = 2\sqrt{2} \left(\frac{T_e + T_i}{4\pi n_{eo} e^2} \right) \frac{c}{\omega_i - \omega_e}$$

is a property of the Vlasov/Maxwell equilibrium. However, in order to determine T_e and T_i it is necessary to proceed to a higher order, i.e.: the Fokker-Planck equation, which

leads to Eq. (11). Eq. (11) does not include sources and sinks that involve fusion reactions and radiation. Approximations employed to estimate Eq. (11) are $v_e \gg v_i,\, V_e,\, V_i$. Source and sink terms added to Eq. (11) give the following result for determination of electron temperature

$$\frac{3}{2} n_{eo} \frac{dT_e}{dt} = \gamma \left\{ n_{\alpha o} \left\langle \frac{dW_\alpha}{dt} \right\rangle_e + \sum_i n_{io} m_i \frac{(V_i - V_e)^2}{t_{ie}} - e\Delta\Phi \sum_i \frac{n_i Z_i}{t_{Fi}} - P_B \right\} = 0 \ . \qquad (37)$$

The second term on the right hand side comes from Eq. (11). It is the heating of electrons by fuel ions. The first term is heating by α-particles. Eq. (11) is not used to evaluate it since it relies on distribution functions described by Eq. (6) whereas α-particles have a slowing down distribution. The lifetime of the α-particles is assumed to be the slowing down time

$$\frac{1}{t_{\alpha s}} = \frac{1}{t_{\alpha e}} + \frac{1}{t_{\alpha 1}} + \frac{1}{t_{\alpha 2}} \ .$$

Eq. (5) is appropriate for $t_{\alpha e}$ and

$$t_{\alpha i} = \frac{2^{3/2}}{8\pi}\, m_i\, \frac{\langle \frac{1}{2} m_\alpha (V_\alpha - V_i)^2 \rangle^{3/2}}{n_{io} Z_\alpha^2 e^4 m_\alpha^{1/2} \ln\Lambda}\, \frac{m_\alpha}{m_i + m_\alpha} \ . \qquad (38)$$

The density of α-particles is estimated from

$$\frac{\partial n_\alpha}{\partial t} = \frac{1}{2} n_1 n_2 \langle \sigma v \rangle - \frac{n_\alpha}{t_{\alpha s}} = 0$$

and

$$\left\langle \frac{dW_\alpha}{dt} \right\rangle_e = \frac{\langle m_\alpha (V_\alpha - V_i)^2 \rangle}{t_{\alpha e}} \ .$$

The third term on the right hand side of Eq. (37) is a sink term due to electrons which escape with fusion product ions (in this case He) to preserve quasi-neutrality. There is a potential barrier for electrons to escape radially - from Eq. (12)

$$\Delta\Phi = -\int_{r_o}^{r_s} E_r\, dr = \int \left[\frac{V_e}{c} B_z - \frac{T_e}{e n_e} \frac{dn_e}{dr} \right] dr > \frac{T_e}{e}$$

(r_s is the radius of the separatrix). However, electrons can also escape in the axial direction where T_e/e should be a reasonable estimate of the potential barrier in a finite system. In addition electrons have kinetic energy, so we assume electrons enter the system with very low energy (same velocity as injected/trapped ions) and leave with $2T_e$. The last term is the Bremsstrahlung power density for which the Svensson formula of Eq. (15) is employed. For the above design parameters

$$\frac{3}{2}\, n_{eo} \frac{dT_e}{dt} = \gamma \left\{ \frac{41}{1 + .756 \times 10^{-7} T_e^{3/2}} + \frac{5.11 \times 10^8}{T_e^{3/2}} - 1.92 \times 10^{-4} T_e - P_B \right\} = 0 \qquad (39)$$

and for $T_e \sim 100$ keV

$$12.4\, \frac{\text{watts}}{\text{cm}^3} + 16.2\, \frac{\text{watts}}{\text{cm}^3} - 19.2\, \frac{\text{watts}}{\text{cm}^3} - 8.3\, \frac{\text{watts}}{\text{cm}^3} \simeq 0 \ ,$$

i.e.: $dT_e/dt = 0$. This is the condition for T_e to be a maximum. It is time dependent but does not vary substantially over a pulse-length of the order of 1 millisec. The largest heating term is heating of electrons by fuel ions. This can be controlled with the applied field B_o. However, if V_e is altered in this way there are other consequences; for example $r_o\Delta r$ increases like $(V_i - V_e)^{-1}$.

Fuel ion temperatures are evaluated by a similar procedure

$$\frac{3}{2}\, n_{io}\frac{dT_i}{dt} = n_\alpha m_\alpha \left\langle \frac{V_\alpha^2}{t_{\alpha i}} \right\rangle - \frac{n_i(T_i - T_e)}{t_{ie}} - \frac{3}{2}\,\frac{T_i n_i}{t_{Fi}} = 0 \ . \tag{40}$$

The second term only comes from Eq. (11) and describes heating of fuel ions by electrons. The last term is a sink term: when a fuel ion fuses it disappears with thermal energy $3T_i/2$. It is replaced by an injected/trapped fuel ion with appropriate V_i but very small thermal energy. The results for T_i are not the same for D and T. However, collisions not explicitly treated would rapidly equalize the temperatures. We take the average for the fuel ion temperature $T_i = 96$ keV. Various equilibrium quantities can now be determined

$$N_e = 2\pi r_o \Delta r n_{eo} = 7.35 \times 10^{17} \text{ cm}^{-1} \ ,$$

$$I = \frac{eN_e}{2\pi r_o}(V_{i\theta} - V_{e\theta}) = 1.42 \times 10^5 \text{ A/cm}$$

and

$$B_m = \sqrt{8\pi n_{eo}(T_e + T_i)} = 88.8 \text{ kG} \ .$$

The maximum magnetic field is $B_o + B_m = 94.7$ kG. The fusion power is given by Eq. (14)

$$P_F = 1.6 \times 10^{-19} n_{1o} n_{2o} \epsilon_F \langle \sigma v \rangle = 864 \text{ watts/cm}^3 \ .$$

This is the peak value. The power/unit length is ($\gamma = 2/3$)

$$\hat{P}_F = 2\pi r_o \Delta r \gamma P_F = 423 \text{ kW/cm} \ .$$

It should be noted that $\langle \sigma v \rangle$ includes the factor 1.5 that is gained from polarizing the fuel ions. The Bremsstrahlung power density and other types of power density can be found in Eq. (39). Several other parameters of interest are

$$L \simeq 2\pi^2 \frac{r_o^2}{c^2} \times 9 \times 10^{17} = 31.5 \ \mu\text{H/cm} \ ,$$

$$R = \frac{(2\pi r_o)^2 m}{N_e e^2}\left(\frac{1}{\tau_{e1}} + \frac{1}{\tau_{e2}}\right) \times 9 \times 10^{17} = .753 \ \mu\Omega\text{/cm}$$

and, thus,

$$\frac{L}{R} = 41.8 \text{ sec} \ .$$

The various power densities previously defined for Engineering analysis are given in Table 2.

Assuming efficiencies $\eta_A = .8$ for the accelerator and $\eta_B = \eta_N = .35$ for thermal conversion the results from Eqs. (16) and (17) are $P_S/P_F = .292$, $P_C/P_F = .075$. The power for sale is $\hat{P}_S = 123.5$ kW/cm and the circulating power is $\hat{P}_C = 31.7$ kW/cm.

Table 2: D-T Power Densities

$P_F = 864$ W/cm^3	$P_E = 19.2$ W/cm^3
$P_P = 12.4$ W/cm^3	$P_B = 8.3$ W/cm^3
$P_D = 16.2$ W/cm^3	$P_R = 35.9$ W/cm^3

Table 3: D-He^3 Reactor Parameters

$n_{eo} = 10^{15}$ cm^{-3}	$n_{1o} = n_{2o} = \frac{1}{3} \times 10^{15}$ cm^{-3}
$\frac{1}{2} m_1 V_1^2 = 450$ keV	$\frac{1}{2} m_2 V_2^2 = 675$ keV
$\langle \sigma v \rangle = 3 \times 10^{-16}$ cm^3/sec	$t_{F1} = t_{F2} = 1/n_i \langle \sigma v \rangle = 10$ sec
$V_e = .44 \times 10^9$ cm/sec	$V_1 = V_2 = .661 \times 10^9$ cm/sec
$r_o = 40$ cm	$B_o = 8.25$ kG
$\omega_1 = \omega_2 = 1.65 \times 10^7$ sec^{-1}	$\omega_e = 1.10 \times 10^7$ sec^{-1}
$\epsilon_F = 18.2$ MeV	$\Omega_o = 3eB_o/(m_1 + m_2) = 4.95 \times 10^7$ sec^{-1}
(protons 14.7 MeV, α-particles 3.5 MeV)	

8.1 D-He^3 Reactor

The data as provided by Table 3 are assumed for the D-He^3 reaction. The electron temperature is determined by

$$\frac{3}{2} n_{eo} \frac{dT_e}{dt} = \gamma \left\{ n_{\alpha o} \left\langle \frac{dW_\alpha}{dt} \right\rangle_e + n_p \left\langle \frac{dW_p}{dt} \right\rangle_e + \sum_{1,2} n_i m_i \frac{(V_i - V_e)^2}{t_{ie}} - 2T_e \sum_i \frac{n_i Z_i}{t_{Fi}} - P_B \right\} = 0 \ . \tag{41}$$

The α-particle heating is small compared to the proton heating. It is reduced compared to the D-T case because the density of α-particles is an order of magnitude less. A factor of 4 comes from the fusion rate and the balance from the reduction of $t_{\alpha s}$ and the product $n_1 n_2$. The slowing down of 14.7 MeV protons by electrons dominates over the fuel ions because of the large energy of the protons compared with the expected electron temperature. The result is that the proton heating is independent of temperature.

$$\begin{aligned} \frac{3}{2} n_{eo} \frac{dT_e}{dt} \ = \ & \gamma \left\{ 19.6 + \frac{4.3 \times 10^8}{T_e^{3/2}} - .32 \times 10^{-4} T_e \right. \\ & - 2.5 \times 10^{-2} T_e^{1/2} \left[1 + 1.78 \left(\frac{T_e}{mc^2} \right)^{1.34} \right. \\ & \left. \left. + 1.27 \frac{T_e}{mc^2} \left(1 + 1.1 \frac{T_e}{mc^2} + \left(\frac{T_e}{mc^2} \right)^2 - 1.25 \left(\frac{T_e}{mc^2} \right)^{2.5} \right) \right] \right\} \ . \end{aligned} \tag{42}$$

Numerically this gives

$$19.6 + 6.1 - 5.44 - 20.3 \simeq 0 \qquad (\text{for } T_e \sim 170 \text{ keV}) \ .$$

Thus the peak temperature is $T_e = 170$ keV and the various power densities in watts/cm^3 as indicated above. The ion temperatures are given by

$$T_i = \left[T_e + \frac{t_{ie}}{n_i} \sum_p n_p m_p \left\langle \frac{V_p^2}{t_{pi}} \right\rangle \right] \Bigg/ \left[1 + \frac{3}{2} \frac{t_{ie}}{t_{Fi}} \right] \ . \tag{43}$$

The average ion temperature is $T_i \simeq 217$ keV. The various equilibrium calculations can now be completed making use of Eq. (25), (26) and (34). $r_o \Delta r = 203$ cm^2 and

$$N_e = 12.75 \times 10^{17} \text{ cm}^{-1} \ ,$$

$$I = 1.75 \times 10^5 \text{ A/cm} \ ,$$

$$B_o + B_m = 121 \text{ kG}$$

and

$$\frac{L}{R} = 195 \text{ sec} \ .$$

The decay time is longer than it was for D-T because the temperature is higher and N_e is larger.

The various power densities for the engineering analysis can be obtained from Eq. (41) and Eq. (14) and are listed in Table 4.

Table 4: D-He^3 Power Densities

$P_F = 98.1$ W/cm^3	$P_E = 5.4$ W/cm^3
$P_P = 19.6$ W/cm^3	$P_B = 20.3$ W/cm^3
$P_D = 6.1$ W/cm^3	$P_R = 6$ W/cm^3

The value for Q is $Q = 4.83$. Assuming $\eta_A = .8$, $\eta_N = .9$ and $\eta_B = .35$ obtains from Eq. (16) and (17) $P_S/P_F = .743$, $P_C/P_F = .154$ as well as $\hat{P}_S = 61.9$ kW/cm and $\hat{P}_C = 12.8$ kW/cm.

Compared with D-T the value of P_F is reduced by a factor of 9 because of the factor of 4 in reactivity and the reduced fuel ion density. However, $\hat{P}_S$ is only reduced by a factor of 2 because of the increased conversion efficiency.

8.3 p-B^{11} Reactor

The data assumed for p-B^{11} is summarized in Table 5.
The equation that determines the electron temperature is

$$\frac{3}{2} n_{eo} \frac{dT_e}{dt} = \gamma \left\{ \frac{14.4}{1 + 1.19 \times 10^{-}7 T_e^{3/2}} + \frac{3.72 \times 10^8}{T_e^{3/2}} - .384 \times 10^{-4} T_e - P_B \right\} = 0 \ .$$

Table 5: p-B^{11} Reactor Parameters

$n_{eo} = 10^{15}$ cm^{-3}	$n_{1o} = .5 \times 10^{15}$ cm^{-3}
$n_2 = 10^{14}$ cm^{-3}	$\langle \sigma v \rangle = 6.4 \times 10^{-16}$ cm^3/sec
$\frac{1}{2} m_1 V_1^2 = 300$ keV	$\frac{1}{2} m_2 V_2^2 = 3.3$ MeV
$t_{F1} = 15.6$ sec	$t_{F2} = 3.12$ sec
$V_e = .661 \times 10^9$ cm/sec	$V_1 = V_2 = .764 \times 10^9$ cm/sec
$\Omega_o = 9.55 \times 10^7$ sec^{-1}	$B_o = 15.3$ kG
$\omega_1 = \omega_2 = 1.91 \times 10^7$ sec^{-1}	$\omega_e = 1.52 \times 10^7$ sec^{-1}
$\epsilon_F = 8.68$ MeV, 3 α-particles	

This holds true numerically if $T_e \simeq 82$ keV, i.e.:

$$3.8 \text{ watts/cm}^3 + 15.8 \text{ watts/cm}^3 - 3.15 \text{ watts/cm}^3 - 16.7 \text{ watts/cm}^3 \sim 0 \ .$$

Eq. (15) is employed for P_B with $\langle Z \rangle = 3$ and $n_e^2 = 10^{30}$. The peak temperature is, thus, $T_e = 82$ keV and the power densities are as indicated. The main point of this calculation is that the electron heating by fuel ions is suppressed by increasing V_e which involves an increase in the external field B_o. The average value of ion temperature calculated by Eq. (43) is 235 keV. The equilibrium quantities are

$$N_e = 13 \times 10^{17} \text{ cm}^{-1} \ ,$$

$$I = 1.27 \times 10^5 \text{ A/cm} \ ,$$

$$B_o + B_m = 96.3 \text{ kG}$$

and

$$\frac{L}{R} = 36 \text{ sec} \ .$$

The power densities are summarized in Table 6. Q for this data is $Q = P_F/P_B = 2.65$.

Table 6: p-B^{11} Power Densities

$P_F = 44.4$ W/cm^3	$P_E = 3.15$ W/cm^3
$P_P = 3.8$ W/cm^3	$P_B = 16.7$ W/cm^3
$P_D = 15.8$ W/cm^3	$P_R = 9.6$ W/cm^3

Assuming $\eta_A = .8$, $\eta_N = .9$ and $\eta_B = .35$ as in the D-He^3 ccalculation gives $P_S/P_F = .509$, $P_C/P_F = .715$, $\hat{P}_S = 19.58$ kW/cm and $\hat{P}_C = 27.5$ kW/cm.

8.4 Comparison of Reactor Parameters

Reactor parameters for D-T, D-He^3 and p-B^{11} are summarized in Table 7. The power can be increased by increasing the density. The scaling with density of the power is relatively simple because all of the power expressions are bilinear in the density. If n_e is increased and the ratios n_1/n_e and n_2/n_e are preserved the expressions for P_F, P_B, P_D, etc. will increase similarly. The limitation is the technology of magnetic fields with super-conducting magnets. To compare the p-B^{11} results with D-He^3 they should involve the same maximum magnetic field. B_m is proportional to $n_{eo}^{1/2}$ and P_F, etc. are proportional to n_{eo}^2. It can thus be inferred that if the electron density is increased by a factor 1.69 (and ratios preserved), the peak magnetic field for the p-B^{11} reaction will also be 121 kG, $P_F = 127$ watts/cm^3 and $P_S = 64.6$ watts/cm^3. Since Δr scales like $n_{eo}^{-1/2}$, $\hat{P}_S$ scales like $n_{eo}^{3/2}$, it follows that $\hat{P}_S = 43.0$ kW/cm and $\hat{P}_C = 60.3$ kW/cm. r_o ccould be increased by a factor of 2 as well as Δr without changing the maximum magnetic field. The result for p-B^{11} would be $\hat{P}_S = 172$ kW/cm. The length of the plasma for a 100 MW reactor would be 5.81 meters. From a physics point of view the simplicity of the reactor design would be in the order D-T, D-He^3 and p-B^{11}. From the point of view of engineering difficulties mainly arising from neutrons the reverse order applies. From the point of view of fuel availability and cost the ordering would be p-B^{11}, D-T, D-He^3. The circulating power is the most serious problem for p-B^{11} since it implies large capital costs. The reason for this is the large design energy of 3.3 MeV for B^{11} in order that the mean velocity will be the same as it is for protons. This velocity $V_i > v_i$, the thermal velocity, is the price paid for confinement. The relative circulating power for D-He^3 is small because of the high temperature of electrons which increases the time for momentum/energy transfer from ions to electrons.

9. CBFR – Mode 2

This mode has been described[13] for p-B^{11} in the Journal "Science". The essential features were noted in section 7.1. The objective is to increase the reactivity $\langle \sigma v \rangle$ by exploiting the resonance and decreasing the circulating power since the particle energies need not be so large, i.e.: $\frac{1}{2}(m_1 V_1^2 + m_2 V_2^2) < 1$ MeV. However, maintaining the ions at the resonance energy $\epsilon_R = \frac{1}{2} m_1 (\mathbf{V}_1 - \mathbf{V}_2)^2$ introduces many effects that could be neglected in mode 1. The ions at different velocities means that ion-ion scattering must be considered. This decreases the momentum transfer time and increases classical diffusion rates for ions. For example with mode 1, ion-ion scattering could be neglected. The diffusion rate is $D_i \sim a_i^2/t_{ie}$, where a_i is the ion gyro-radius and t_{ie} is the momentum transfer time from ions to electrons. $t_{ie} \sim 1$ sec and $a_i \sim 1$ cm for the largest magnetic field. The diffusion time for an ion is $\tau_{Di} \simeq (\Delta r/a_i)^2 t_{ie} \sim 25$ sec (assuming $\Delta r \simeq 5$ cm) which is longer than the fusion time. For p-B^{11} with $n_1 = .5 \times 10^{15}$, $n_2 = 10^{14}$, $\epsilon_R \simeq 600$ keV the slowing down time for protons would be $t_{12} \simeq .2$ sec, $\tau_{Di} \sim 5$ sec which is less than the fusion time even if $\langle \sigma v \rangle$ increases by a factor of 2. The momentum transfer time due to ion-ion collisions would also increase the dissipated power P_D and the circulating power. These problems can be minimized by reducing the B^{11} density but that also reduces the Fusion power. A quantitative investigation is needed to evaluate the merits of mode 2. The accuracy of such an investigation is limited because classical diffusion theory has not been developed for the FRC configuration. All

[13] N. Rostoker, M. Binderbauer and H.J. Monkhorst, *Science* **278**, 1419, 1997.

Table 7: Design and Performance of Mode 1 Reactors

	D-T	D-He^3	p-B^{11}
Densities [cm^{-3}] ($n_e = 10^{15}$ cm^{-3})			
n_1	$.5 \times 10^{15}$	$.5 \times 10^{15}$	$.5 \times 10^{15}$
n_2	$.5 \times 10^{15}$	$.5 \times 10^{15}$	10^{14}
Fuel Ion Energy [keV]			
$\frac{1}{2} m_1 V_1^2$	800	450	300
$\frac{1}{2} m_2 V_2^2$	450	675	3300
Reactivity $\times 10^{-16}$ [cm^3/sec]	12	3.0	6.4
Fusion Energy [MeV]	17.4	18.2	8.68
Temperatures [keV]			
T_i	96	217	235
T_e	100	170	82
Current I $\times 10^5$ [A/cm]	1.42	1.75	1.27
Magnetic Field [kG]			
B_o	5.88	8.25	15.3
$B_o + B_m$	94.7	121	96.3
Decay Time L/R [sec]	41.8	195	36
Fusion Power/Radiation Q	104	4.83	2.65
Power for Sale/Fusion Power	.292	.743	.509
Circulating Power/Fusion Power	.075	.154	.715
Power for Sale $\hat{P}_S$ [kW/cm]	123	61.9	19.6
Circulating Power $\hat{P}_C$ [kW/cm]	31.7	12.8	27.5

previous classical treatments of transport assume that $a_i \ll n_i/|\boldsymbol{\nabla} n_i|$ which is not the case for the FRC particularly in the region where B_z is small and the density is largest. This inequality is only satisfied where the magnetic field is largest and the density much less than the peak density. The diffusion velocity $V_{Di} \sim D_i|\boldsymbol{\nabla} n_i|/n_i$ should be far from constant. V_{Di} should be large where the density is large and the fusion time a minimum and small where the density is small. The conservation of energy expressed by Eq. (9) has some additional

terms if diffusion is considered

$$\frac{d}{dt}\left[\left(\sum_i \frac{1}{2}\, n_i m_i V_{i\theta}^2\right) + \frac{B_z^2}{8\pi}\right] = -\frac{n_1 m_1}{t_{12}}\left(V_{1\theta} - V_{2\theta}\right)^2 - \frac{n_1 m_1}{t_{1e}}\left(V_{1\theta} - V_{e\theta}\right)^2 + \sum_{i=1,2} n_i V_{ir}\left[e_i E_r - \frac{T_i}{n_i}\frac{dn_i}{dr}\right] , \tag{44}$$

$$V_{ir} = -\frac{D_i}{n_i}\frac{\partial n_i}{\partial r}$$

where

$$D_1 \sim \frac{a_1}{t_{12}} , \qquad \frac{1}{L_1} = \frac{1}{n_1}\frac{\partial n_1}{\partial r} .$$

The last term was previously omitted although it is of the collisional order. From the equilibrium equation, Eq. (12)

$$n_i e_i E_r - T_i \frac{dn_i}{dr} = -\frac{n_i e_i}{c} V_{i\theta} B_z - n_i m_i \frac{V_{i\theta}^2}{r} \simeq -n_i m_i \Omega_i V_{i\theta} . \tag{45}$$

After integrating Eq. (44) the result is

$$\frac{d}{dt}\left(\sum_i \frac{1}{2}\, N_i m_i V_i^2 + \frac{1}{2}\, L I^2\right) = -\frac{N_1 m_1}{\tau_{12}}\left(V_{1\theta} - V_{2\theta}\right)^2 - \frac{N_1 m_1}{\tau_{1e}}\left(V_{1\theta} - V_{e\theta}\right) + \int_0^{r_B} 2\pi r dr \frac{n_1 m_1}{t_{12}}\left(\frac{a_1}{L_1}\, V_{1\theta}^2 + \frac{a_2}{L_2}\, V_{2\theta}^2\right) . \tag{46}$$

The last term in Eq. (45) has been omitted because it is almost an even function of $r^2 - r_o^2$ and V_{ir} is an odd function so that the contribution to Eq. (46) is of order $\Delta r/r_o$. For conventional transport theory $a_i/L_i \ll 1$. This is not the case particularly where the density is large. The right hand side of Eq. (46) is the dissipation and would be dominated by the first term that involves collisions between p and B^{11} ions. However, the last term is of the same order of magnitude and opposite sign. A quantitative result requires an extension of transport theory which is in progress. The dissipated power P_D and the replacement power P_R determine the circulating power P_C. If the fuel ion energies are reduced compared to mode 1, P_R would decrease as would P_D provided that the terms involving t_{12} nearly cancel. If they do not nearly cancel, the circulating power[14] P_C to maintain the resonance would be much too large. The determination of ion temperatures is important because if they are too large, the resonance will be wiped out. The electron temperature is particularly important because $Z = 5$ for Boron so that Bremsstrahlung can become excessive. Consider the determination of electron temperature as defined by Eq. (10) and (11)

$$\frac{3}{2}\, n_{eo}\frac{dT_e}{dt} = \gamma\left\{\frac{n_e m (V_1 - V_e)^2}{t_{e1}} + \frac{n_e m (V_e - V_2)^2}{t_{e2}}\right\} . \tag{47}$$

This result is entirely due to scattering. It is apparent from Eq. (11) that the drag term contribution from $\langle \Delta v \rangle_i$ is much smaller. However, the definition of temperature from Eq. (10)

$$\frac{3}{2}\, T_e = \frac{1}{2}\, m\left[\langle v^2 \rangle_e - V_e^2\right]$$

[14] A. Carlson, *Science* **281**, 3072, 1998.

implies that if $V_e \simeq$ constant as is expected for a steady state or nearly constant in a periodic state, then

$$\frac{3}{2}\frac{dT_e}{dt} \simeq \frac{m}{2}\frac{d}{dt}\langle v^2\rangle_e \ .$$

The result from this calculation is

$$\frac{3}{2}\, n_{eo}\frac{dT_e}{dt} = \gamma\left\{\frac{n_e m V_1(V_1 - V_e)}{t_{e1}} - \frac{n_e m V_2(V_e - V_2)}{t_{e2}}\right\} \ . \tag{48}$$

Eq. (11) is replaced by

$$\frac{3}{2}\, N_e\frac{dT_e}{dt} = m\int 2\pi r\, dr \int d\mathbf{v}\left[\mathbf{v}\cdot\langle\Delta\mathbf{v}\rangle_e + \frac{1}{2}\,\mathrm{tr}\,\langle\Delta\mathbf{v}\Delta\mathbf{v}\rangle_e\right] f_e - e\int 2\pi r\, dr\, n_e(\mathbf{V}_e\cdot\mathbf{E}) \ . \tag{49}$$

In this case the drag term involving $\langle\Delta v\rangle_e$ is important. It is also necessary to consider how the electron velocity V_e is maintained at a nearly constant value and whether the external influences that accomplish this will contribute to dT_e/dt. For example if a steady state is maintained for fuel protons by injecting a low density beam at higher energy to replace protons that undergo fusion and also drive the fuel protons so that they don't slow down, then its effect on temperature must be considered by adding additional terms to $\langle\Delta v\rangle_e$ and $\langle\Delta v\Delta v\rangle_e$. If pulsed drive as previously discussed is employed then the last term of Eq. (49) must be considered which involves $V_{e\theta}$ and $E_\theta = -(L/2\pi r_o)(dI/dt)$. In the former case the driver beam has very low density compared to the fuel protons so that the effect on electron temperature would be a small correction. In the latter case E_θ changes sign, n_e and V_e are almost constant so the average value over a period is zero.

Similar considerations apply to protons. Subject to the assumption of Maxwell distributions for all particles and $(V_1 - V_2) \gg v_1, v_2,\ v_e \gg V_1, V_2, v_1, v_2$

$$\frac{3}{2}\, n_{1o}\frac{dT_1}{dt} = \gamma\left\{\frac{3\, n_{1o}(T_e - T_1)}{t_{1e}} - \frac{n_1 m_1 V_2(V_1 - V_2)}{t_{12}} + e\int 2\pi r\, dr\, n_1(\mathbf{V}_1\cdot\mathbf{E})\right\} \ . \tag{50}$$

If the velocity V_1 is maintained by an auxiliary beam which is also treated as Maxwellian the result would be

$$\frac{3}{2}\, n_{1o}\frac{dT_1}{dt} = \gamma\left\{\frac{3\, n_{1o}(T_e - T_1)}{t_{1e}} + \frac{n_{1o} m_1 (V_1 - V_2)^2}{t_{12}}\right\} \ .$$

However, the driver beam because of the low density would not have a Maxwell distribution, but a slowing down distribution so that this result is not acceptable. The correct result will require a detailed numerical calculation. If the pulsed drive is employed the last term of Eq. (50) may be negligible for the same reasons as in the discussion of electron heating. Alternative models for the calculation of temperatures have been employed by W. Nevins[15] and by M. Lampe and W. Mannheimer[16].

[15]W.M. Nevins, *Science* **281**, 3072, 1998.

[16]M. Lampe and W. Mannheimer, Naval Research Laboratory Report NRL/MR/6709-98-8305, Oct. 30, 1998.

10. Technology

10.1 Ion Beams

Beams of neutral atoms or neutralized ion beams could be employed. They could be steady state or pulsed. The present status of the technology favors pulsed neutralized ion beams. Steady state accelerators to produce neutrals at 100's of keV must first accelerate negative ions and then ionize them. Such accelerators exist but they are too large for the CBFR since they were developed for tokamaks. Pulsed negative ion diodes have been developed at UCI and Lebedev Institute, but this technology is new and no longer supported. In addition ionization of neutrals by the fuel plasma places substantial limitations on the design. The fuel plasma Δr must be much larger. The pulsed positive ion diode technology is quite advanced and a considerable amount of research has been carried out on the propagation of neutralized ion beams[17] in plasma, across magnetic fields etc. Single pulse machines that produce 100's of kiloamps at 100's of kilovolts for 100-150 nsec have been available for some time. The average current requirements are $I = \frac{2}{3}\sum_{i=1,2}(N_i/t_{Fi})Z_i e \simeq 1$ A/meter for replacing the burnt fuel. For a rep-rate of 1 kHz the required current of each pulse is 10 kA which is well within the present technology for single pulses. In recent years a rep-rate technology has been developed for materials processing. Q.M. Technologies markets a QM-1 modulator system that produces 200 kV, 80 kA, 150 nsec pulses with a rep-rate of 10 Hertz. The technologies involved were developed at Sandia Laboratories and Cornell University. This technology requires further development, but the requirements for fusion reactors are within reach. They are not compact which is not important for civilian applications. They could be made compact by power conditioning of the output of direct converters to accommodate the accelerators.

10.2 Polarized Fuel

Polarization of fusion fuel increases the fusion cross section by a factor of 1.5 for D-T and D-He^3 and by a factor of 1.6 for p-B^{11}.

Polarization of nuclear spins with optical pumping techniques applied to atoms has a long history.[18] It is very well understood theoretically and has been applied to a large number of atoms. A classical review on the subject was written by Happer.[19] Although now over twenty-five years old, it is still considered up-to-date and definitive. A most recent, very accessible relevant monograph is that by Suter.[20]

Polarized ion and atomic beams have been used extensively in nuclear physics. It has been recognized for a long time that laser-driven optical pumping polarization is the technique of choice, whenever applicable. Its simplicity, speed and high polarization achievable make it most attractive. A 1993 Conference Proceeding[21] gives a good status report. Milliampère currents (or about 10^{16}/sec) highly polarized H, D, He^3, Li^6, Li^7 and their ions are produced rather routinely. For our purpose, later work by Coulter *et al.*[22] and Stenger *et*

[17] F.J. Wessel, A. Fisher, H.U. Rahman, J.J. Song and N. Rostoker, *Phys. Fluids B* **2**(6), 1467, 1990.

[18] A. Kastler, *J. Phys. Radium* **11**, 225, 1950.

[19] W. Happer, *Rev. Mod. Phys.* **44**, 169, 1972.

[20] D. Suter, *The Physics of Laser-Atom Interactions*, Cambridge UP, 1997.

[21] AIP Conference Proceeding 293, *Polarized Ion Sources and Polarized Gas Targets*, Madison WI 1993, AIP Press, 1994.

[22] K.P. Coulter *et al.*, *Phys. Rev. Lett.* **68**, 174, 1992.

al.[23] has shown that current increases by two orders of magnitude (to at least 4×10^{17}/sec) of polarized hydrogen is easily achieved with the so-called spin exchange optical pumping technique. Our studies and consultation of experts have convinced us that this technique can be scaled up to the required production of 10^{20}/sec spin polarized hydrogen atoms. The laser power requirement should reach several tens of kWatts, which is not exorbitant by modern standards.

Probably because of lack of a motivation, no polarization of the B^{11} nucleus has been attempted thus far. We have begun a simulation study of applicable techniques to achieve high-rate, high efficiency B^{11} nuclear polarization. A direct optical pumping technique with appropriately tuned KrF lasers using inverse Raman or Brillouin shifts has been considered first. According to Happer (private communication), this scheme should work, and according to NRL laser experts Bodner and Lehmberg (private communication), pulsed laser power requirements are achievable, and possibly commercially available. Results of beam, laser and efficiency optimizations will be published.[24]

Depolarization has been studied[25] for FRC's. Depolarization by plasma waves was found to be unlikely because of the dramatically varying precession frequencies of the spins as the fuel ions oscillate through the null surface of the betatron orbits.

10.3 Direct Energy Conversion of Bremsstrahlung X-Rays

The CBFR plasma will have electron temperatures $T_e \sim 100 - 200$ keV. According to theory, the Bremsstrahlung power spectrum behaves approximately as $\exp(-E_x/T_e)$, with E_x the X-ray photon energy. Therefore, most of the energy is radiated as X-rays with $E_x \leq T_e$.

Practically all fusion devices accept Bremsstrahlung power as a loss. So far we considered a thermal conversion of this power through its absorption in the fusion chamber's first wall as heat. It is hard to imagine achieving better than 35% efficiency with this conversion process because we can not reach or sustain extremely high cooling liquid temperatures.

There is, however, a possibility to convert the X-ray power directly into electricity by exploiting the photo-electric effect. This has been suggested by Tajima and Mima (TM)[26]. In the CBFR the X-rays hit the first wall with momenta that are largely normal to its surface. TM propose to cover this wall with a multiply layered material that consists of high-Z and low-Z metal films alternatingly stacked with an insulating low-Z film or vacuum gap in-between. The high-Z films are electrically connected, and so are the low-Z metal films. X-rays will photo-ionize K shells, mostly of the high-Z metal, with electrons emitted largely forward and normal to the films. The films are thin relative to the stopping range for the photoelectrons (with energies on the order of 100 keV). The low-Z metal films will then get a negative potential relative to the high-Z films: electric power is extracted. The integrated thickness of the high-Z films is larger than the mean free path for the X-ray photon absorption. The high-Z films should have a thickness on the order of 10 to 100 μm, whereas the low-Z films can be thicker to sustain voltages on the order of tens of keV. For

[23] J. Stenger *et al.*, *Phys. Rev. Let.* **78**, 4177, 1997.

[24] T. Waddington and H.J. Monkhorst, to be published.

[25] H.J. Monkhorst, M.W. Binderbauer and N. Rostoker, Conference on *Current Trends in International Fusion Research*, March 10-14, 1997, Washington DC – to be published in the Proceedings by Plenum Press, Edited by E. Panarella.

[26] T. Tajima and K. Mima, private communication.

high-Z metals such as tungsten only a few layers should be sufficient. By properly adjusting the parameters that define the layered structure (choices of high-Z, low-Z metals; thickness of films; materials between metal films; number of layers). TM expect efficiencies of 60%, or even higher for higher X-ray energies in the CBFR. The physics of this converter was used previously in the construction of a X-ray detector by Narusa and Matayama.[27]

Major advantages seem to be the simplicity, the possibility to cover the entire inner surface of the reactor, expected ease of manufacturing of the layered material and the small overall thickness on the order of a centimeter. By properly alloying the films we can taylor the conductive, thermal and mechanical properties to our needs.

For p-B^{11} fuel the Bremsstrahlung is most important and the increase in efficiency would make a significant increase in P_S.

9. Acknowledgement

This research was supported by the Office of Naval Research, the University of California and the University of Florida.

[27]Y. Narusa and T. Hatayama, in *Transducers '87, 4th Int. Conf. on Solid-State Sensors and Actuators.*